Role of Structural and Functional Elements of Mouse Methionine-*S*-Sulfoxide Reductase in Its Subcellular Distribution[†]

Hwa-Young Kim and Vadim N. Gladyshev*

Department of Biochemistry, University of Nebraska, Lincoln, Nebraska 68588

Received January 19, 2005; Revised Manuscript Received March 3, 2005

ABSTRACT: Oxidized forms of methionine residues in proteins can be repaired by methionine-*S*-sulfoxide reductase (MsrA) and methionine-*R*-sulfoxide reductase (MsrB). In mammals, three MsrBs are present, which are targeted to various subcellular compartments. In contrast, only a single mammalian MsrA gene is known whose products have been detected in both cytosol and mitochondria. Factors that determine the location of the protein in these compartments are not known. Here, we found that MsrA was present in cytosol, nucleus, and mitochondria in mouse cells and tissues and that the major enzyme forms detected in various compartments were generated from a single-translation product rather than by alternative translation initiation. Both cytosolic and mitochondrial forms were processed with respect to the N-terminal signal peptide, and the distribution of the protein occurred post-translationally. Deletion of amino acids 69−108, 69−83, 84−108, or 217−233, which contained elements important for MsrA structure and function, led to exclusive mitochondrial location of MsrA, whereas a region that affected substrate binding but was not part of the overall fold had no influence on the subcellular distribution. The data suggested that proper structure−function organization of MsrA played a role in subcellular distribution of this protein in mouse cells. These findings were recapitulated by expressing various forms of mouse MsrA in *Saccharomyces cerevisiae*, suggesting conservation of the mechanisms responsible for distribution of the mammalian enzyme among different cellular compartments.

Methionine residues in proteins can be readily oxidized to methionine sulfoxides (Met-SO)[1] by reactive oxygen species (reviewed in refs *1*−*4*). To repair proteins from such damage, most organisms employ Met-SO reductases, which reduce Met-SO to Met (*5*, *6*). Two distinct enzymes, MsrA and MsrB, are responsible for Met-SO reduction and act on individual diastereomers of Met-SO. MsrA is specific for the *S* isomer of Met-SO (methionine-*S*-sulfoxide, Met-*S*-SO) (*7*−*12*), whereas MsrB can only reduce the *R* form of this amino acid (methionine-*R*-sulfoxide, Met-*R*-SO) (*13*−*19*).

We recently reported that human and mouse genomes possess three MsrB genes that code for MsrB1, MsrB2, and MsrB3 (*20*). MsrB1 (also known as selenoprotein R and selenoprotein X) (*15*, *21*) had an active-site selenocysteine and was present in the cytosol and nucleus. The other two mammalian MsrBs contained cysteine in place of selenocysteine. MsrB2 (also known as CBS-1) (*14*, *22*) resided in mitochondria. Human MsrB3 occurred in two protein forms, MsrB3A and MsrB3B, which were generated by alternative first exon splicing. MsrB3A was targeted to the endoplasmic reticulum (ER), and MsrB3B was targeted to mitochondria (*20*). In contrast to human MsrB3, we found no evidence for alternative splicing in the mouse MsrB3 gene. Instead, the ER signal was located upstream of the mitochondrial signal sequence in a single coding region, whose product was targeted to the ER (*23*). These observations suggested that different cellular compartments in mammals maintain a system for repair of oxidized methionine residues.

In contrast to the three MsrBs, mammals contain only a single MsrA gene (*10*, *11*). This protein has a predicted N-terminal mitochondrial signal peptide. Recently, Hansel et al. reported that a green fluorescent protein (GFP)-fused human MsrA, when transfected into mammalian cells, localized to mitochondria (*24*). However, Vougier et al. provided evidence that MsrA was located in both mitochondria and cytosol by purifying rat liver MsrA from these fractions followed by characterization of enzyme preparations (*25*). It is not known how MsrA could be targeted to both cytosol and mitochondria and what possible determinants are for its subcellular distribution. Also not known is whether MsrA resides in additional cellular compartments.

In the present study, we examined cellular distribution patterns of mouse MsrA using subcellular fractionation of tissue samples expressing various MsrA forms and by immunofluorescence detection of MsrA and GFP-fused MsrA expressed in transfected cells. Our data revealed that mouse MsrA is localized in cytosol, nucleus, and mitochondria. We found that proper structure−function organization of MsrA was a key factor for dual targeting of this protein in mitochondria and cytosol. In addition, same factors determined the subcellular distribution of mouse MsrA when it was expressed in yeast cells. These data are discussed with

[†] This study was supported by NIH AG021518 (to V.N.G.).

* To whom correspondence should be addressed: N151 Beadle Center, Department of Biochemistry, University of Nebraska, Lincoln, NE 68588. Telephone: 402-472-4948. Fax: 402-472-7842. E-mail: vgladyshev1@unl.edu.

[1] Abbreviations: Met-SO, methionine sulfoxide; Met-*R*-SO, methionine-*R*-sulfoxide; Met-*S*-SO, methionine-*S*-sulfoxide; GFP, green fluorescent protein; DTT, dithiothreitol; LC−MS/MS, liquid chromatography−tandem mass spectrometry.

10.1021/bi0501131 CCC: $30.25
Published on Web 05/10/2005

respect to the mechanisms responsible for distribution of mouse MsrA among cellular compartments.

MATERIALS AND METHODS

Preparation of Recombinant Mouse MsrA Proteins. The mouse MsrA cDNA was amplified from a mouse EST clone (ID 1381477, GenBank accession number AI037485, Open Biosystems) and cloned into the *Nde*I/*Xho*I sites of pET21a (Novagen) to code for a protein with a C-terminal His tag, resulting in a plasmid designated pET-MsrA(L)-His. The MsrAΔ(1−46)-His construct, which lacked 46 N-terminal amino acids and coded for a polypeptide containing amino acids 47−233 of mouse MsrA linked to a C-terminal His tag, was made by inserting the corresponding cDNA into the *Nde*I/*Xho*I sites of pET21a. All constructs were verified by DNA sequencing. MsrA proteins were expressed in *Escherichia coli* BL21(DE3) cells, purified using TALON metal-affinity resin (Clontech), and analyzed for purity by SDS−PAGE. Protein concentrations were determined by the Bradford method using bovine serum albumin as a standard. We also generated full-length MsrA and MsrAΔ(1−46) constructs without His tag using a pET21b.

Determination of MsrA Activity and Analysis of Enzyme Kinetics. MsrA activity was assayed using dabsylated L-Met-*S*-SO as the substrate. A typical reaction mixture (100 μL) for reduction of dabsyl-Met-*S*-SO to dabsyl-Met contained 50 mM sodium phosphate (pH 7.5), 50 mM NaCl, 20 mM dithiothreitol (DTT), 200 μM dabsyl-Met-*S*-SO, and 1 μg of purified proteins. The reaction was carried out at 37 °C for 30 min and stopped by adding 200 μL of acetonitrile. The reaction product, dabsyl-Met, was analyzed by HPLC as described previously (*16*). K_m and k_{cat} values were determined using Lineweaver−Burk plots.

Isolation of Mitochondria from Mouse Tissues and Transfected Cells. Mitochondria were isolated from mouse tissues using a mitochondria isolation kit (Sigma) following the protocol of the manufacturer. All procedures were performed at 4 °C. Briefly, 0.2 g of fresh mouse brain, liver, or kidney tissues were rinsed with extraction buffer (10 mM Hepes at pH 7.5, 200 mM mannitol, 70 mM sucrose, and 1 mM EGTA), cut into pieces, and homogenized with the extraction buffer containing 2 mg/mL albumin using a Dounce homogenizer. The homogenate was centrifuged at 600*g* for 5 min. The supernatant was further centrifuged at 11000*g* for 10 min. The resulting supernatant, corresponding to the cytosolic fraction, was transferred to a new tube and kept at −20 °C. The pellet was resuspended in the extraction buffer and centrifuged at 600*g* for 5 min. The supernatant was then again centrifuged at 11000*g* for 10 min. Finally, the pellet was resuspended in a storage buffer (10 mM Hepes at pH 7.4, 250 mM sucrose, 1 mM ATP, 0.08 mM ADP, 5 mM sodium succinate, 2 mM K_2HPO_4, and 1 mM DTT) and designated as the mitochondrial fraction. The isolated fractions were analyzed for purity by Western blotting using anti-porin antibodies (Molecular Probes) as a mitochondrial marker and anti-thioredoxin reductase 1 antibodies as a cytosolic marker.

To isolate mitochondria from NIH 3T3 cells transfected with the MsrA-His (C-terminal His-tag) construct, the 24 h post-transfection cells were collected by scrapping, washed twice with PBS, resuspended in the above extraction buffer containing 2 mg/mL albumin and proteinase inhibitor cocktail (Roche), and homogenized using a Dounce homogenizer. The mitochondria were isolated as described above and resuspended in the extraction buffer.

Constructs for Subcellular Localization in Mammalian Cells. GFP fusion expression constructs for examining subcellular localization of MsrA were prepared using pEGFP-N1 (Clontech). The sequences that code for the initial 46 amino acids (including the mitochondrial target peptide) and the full-length (amino acids 1−233) mouse MsrA were cloned into the *Xho*I/*Eco*RI sites of pEGFP-N1, resulting in MsrA(1−46)-GFP and MsrA-GFP, respectively. MsrAΔ(1−46)-GFP (amino acids 47−233 of MsrA) was obtained by cloning the corresponding PCR-amplified fragment into the *Xho*I/*Eco*RI sites of pEGFP-N1. MsrAΔ(69−108)-GFP construct (deletion of 69−108 amino acids of MsrA) was generated using QuickChange Site-Directed Mutagenesis Kit (Stratagene) as described (*26*).

To create MsrA-only expression construct (without GFP), the full-length PCR fragment of MsrA was cloned into the *Xho*I/*Bsr*GI sites of pEGFP-N1 that lacked the GFP coding sequences. The resulting construct was designated as MsrAΔGFP. Other MsrA mutant constructs including MsrAΔ(24−46)ΔGFP, MsrAΔ(69−108)ΔGFP, MsrAΔ(69−83)ΔGFP, MsrAΔ(84−108)ΔGFP, and MsrAΔ(217−233)ΔGFP were made according to a procedure previously described (*26*).

To generate a C-terminal His-tag MsrA expression construct, a PCR was carried out using pET-MsrA(L)-His as a template. The full-length C-terminal His-tagged PCR fragment was cloned into the *Eco*RI/*Bsr*GI sites of pEGFP-N1 that lacked the GFP coding sequences. The resulting construct was designated MsrA-His and contained additional 8 residues (LEHHHHHH) at the C terminus.

Fluorescence Confocal Microscopy. Transfections into monkey kidney CV-1 cells or mouse fibroblast NIH 3T3 cells with appropriate constructs were performed using Lipofectamine (Invitrogen). Mitochondria were stained with MitoTracker Red (Molecular Probes). For immunofluorescence staining of MsrA, cells were treated with methanol at −20 °C for 30 s, washed twice with PBS buffer, and fixed with fresh 4% *para*-formaldehyde in PBS buffer for 5 min at room temperature. MsrA proteins were stained with polyclonal anti-rat MsrA antibodies (kindly provided by Bertrand Friguet) followed by secondary anti-rabbit Cy5-conjugated antibodies (Jackson ImmunoResearch Laboratories). Images were collected using a BioRad MRC1024ES laser scanning microscope.

Constructs for Subcellular Localization in Saccharomyces cerevisiae. The constructs for subcellular location of mouse MsrA proteins in yeast cells were prepared using a yeast expression vector p423 GPD (*27*). Full-length MsrA, MsrAΔ(69−108), MsrA(21−233), and full-length MsrA with a C-terminal His tag were PCR-cloned into the *Bam*HI/*Sal*I sites of p423.

Isolation of Mitochondria from S. cerevisiae Cells Expressing Mouse MsrA Forms. The constructs were transformed into *S. cerevisiae* GY4 cells (*MATa his3 leu2 met15 ura3 ΔmsrA::URA3*) lacking the yeast MsrA gene (*15*), and the transformants were selected for histidine prototrophy. Cells containing p423 only, mouse full-length MsrA, MsrAΔ(69−108), or MsrA(21−233) were grown aerobically at 30

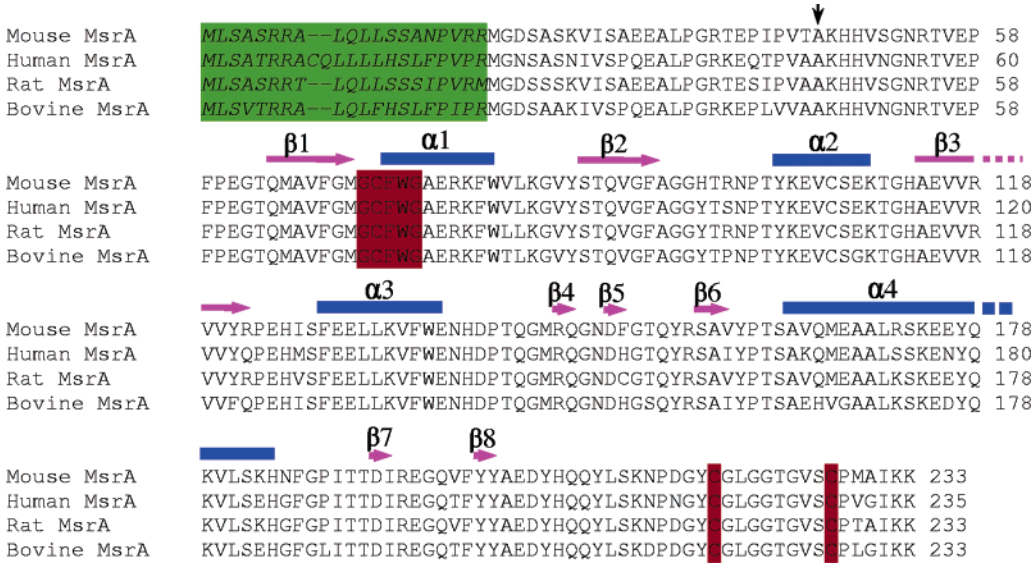

FIGURE 1: Alignment of mammalian MsrA sequences. Secondary-structure elements are indicated above sequences based on the bovine MsrA structure (*9*). The active-site GCFWG motif and Cys218 and Cys227 residues are highlighted in red. The predicted mitochondrial signal peptides are shown in italics and highlighted in green. The end of the first exon is indicated by an arrow.

°C in a synthetic minimal medium (0.37% yeast nitrogen base without amino acids and ammonium sulfate, 0.3% ammonium sulfate, 0.1% K_2HPO_4, 0.077% complete supplement mixture without histidine) supplemented with 2% D,L-lactate as a nonfermentable carbon source. The medium was adjusted to pH 5.0 with KOH.

Mitochondria were isolated as described previously (*28*). The cells grown in stationary phase were harvested and washed once with distilled water. The pellet was resuspended in 0.1 M Tris-HCl at pH 9.4 and 10 mM DTT (0.4 g wet weight/mL) and incubated at 30 °C for 30 min. The suspension was washed once with 1.2 M sorbitol and resuspended in 1.2 M sorbitol and 20 mM potassium phosphate at pH 7.4 (0.15 g wet weight/mL) containing lyticase (5 mg/g cell, Sigma). The suspension was incubated at 30 °C with gentle shaking for 1 h to generate spheroplasts. The spheroplasts were harvested by centrifugation at 1500*g* for 5 min at room temperature, washed twice with 1.2 M sorbitol, and homogenized in an extraction buffer (0.6 M mannitol and 10 mM Tris-HCl at pH 7.4) containing 1 mM phenylmethylsulfonyl fluoride and 1 mg/mL albumin using a Dounce homogenizer. The homogenate was centrifuged at 3000*g* for 5 min. The supernatant was further centrifuged at 9000*g* for 10 min. The resulting supernatant, corresponding to the cytosolic fraction, was transferred to a new tube. The pellet was resuspended in the extraction buffer and centrifuged at 3000*g* for 5 min. The supernatant was then again centrifuged at 9000*g* for 10 min. The pellet was washed twice with the extraction buffer, resuspended in the extraction buffer, and designated as the mitochondrial fraction. The purity of each fraction was monitored by Western blots using anti-porin antibodies (Molecular Probes) for a mitochondrial marker and anti-3-phosphoglycerate kinase antibodies (Molecular Probes) for a cytosolic marker. The cytosolic fractions were shown to be pure. The mitochondrial fractions were slightly contaminated with cytosol.

Purification of Mitochondrial and Cytosolic Mouse MsrA Forms from S. cerevisiae. The GY4 cells containing C-terminal His-tagged MsrA were grown at 30 °C in the above synthetic medium and harvested in stationary phase. The mitochondria and cytosol were isolated as described above. The final mitochondrial fraction was resuspended in PBS and treated by sonication. The proteins were purified using TALON metal-affinity resin.

Western Blotting. Cell extracts transiently transfected with appropriate constructs were prepared using CelLytic-M (Sigma) lysis buffer. The polyclonal anti-GFP antibodies (Invitrogen) were used to detect GFP-fused MsrA proteins. The polyclonal antibodies against rat MsrA were used to detect GFP-fused MsrA or recombinant MsrA proteins from transfected mammalian and yeast cells and endogenous MsrA from mouse tissues. The polyclonal anti-His antibodies (Rockland Immunochemicals) were used to detect His-tagged MsrA proteins from transfected cells.

Mass Spectrometry. The purified cytosolic and mitochondrial MsrA proteins were subjected to SDS−PAGE. The bands corresponding to MsrA were excised and subjected to digestion with trypsin. Liquid chromatography−tandem mass spectrometry (LC−MS/MS) was performed with a quadrupole time-of-flight mass spectrometer (Micromass) using electrospray ionization. Peptides were identified using Mascot software program (Matrix Science, http://www.matrixscience.com/).

RESULTS

Occurrence of Mitochondrial and Cytosolic Forms of MsrA in Mouse Tissues. Human and mouse genomes contain three MsrB genes that code for MsrB1 (selenoprotein R; cytosolic and nuclear protein), MsrB2 (CBS-1; mitochondrial protein), and MsrB3 (ER and mitochondrial forms in humans; ER form in mice) (*14*, *15*, *20*, *23*, *29*). In contrast, there is only one MsrA gene in mammals (*10*, *11*). Recent studied revealed that human MsrA was targeted to mitochondria (*24*) and that rat MsrA localized to both mitochondria and cytosol (*25*). All mammalian MsrAs contain a predicted mitochondrial signal peptide consisting of a typical amphipathic presequence (Figure 1). These findings raised questions about which compartments contain MsrA in other animals, how the mitochondrial and cytosolic forms of MsrA are generated,

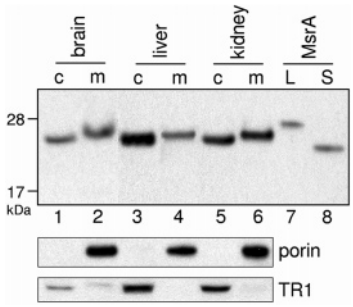

FIGURE 2: Mitochondrial and cytosolic forms of MsrA in mouse tissues. Mitochondrial and cytosolic fractions were isolated from adult mouse brain, liver, and kidney as described in the Materials and Methods. Polyclonal anti-MsrA antibodies were used for protein detection. Porin and thioredoxin reductase 1 (TR1) were used as mitochondrial and cytosolic markers, respectively, and were detected with the corresponding antibodies. Lane 1, brain cytosolic fraction; lane 2, brain mitochondrial fraction; lane 3, liver cytosolic fraction; lane 4, liver mitochondrial fraction; lane 5, kidney cytosolic fraction; lane 6, kidney mitochondrial fraction; lane 7, full-size MsrA expressed in *E. coli*; and lane 8, MsrAΔ(1−46) expressed in *E. coli*.

and whether additional MsrA forms (such as a possible ER-resident or nuclear form) are also present in mammalian cells.

To test if various MsrA forms are present in mouse tissues as well as to characterize subcellular distribution of these forms, we isolated mitochondrial and cytosolic fractions from adult mouse brain, liver, and kidney and subjected them to Western blot analysis with antibodies specific for MsrA (Figure 2). We also expressed in *E. coli* a full-size MsrA form and an MsrAΔ(1−46) form that lacked sequences encoded by the first exon and used these proteins as controls to determine the size of various MsrA forms.

Mouse MsrA proteins were present in both mitochondrial and cytosolic fractions in all tissues tested. The MsrA form detected in the cytosol was slightly smaller than that detected in mitochondria. This observation was consistent with the occurrence of two rat MsrA forms and with the observation that the rat mitochondrial MsrA form was also slightly larger than the cytosolic form (*25*). It should be noted that both rat liver forms had sequences corresponding to exon 1 identified by MS/MS analysis (*25*), which suggests against alternative first exon splicing as a mechanism for generation of these forms.

We observed that both cytosolic and mitochondrial mouse MsrA forms were smaller than the full-size MsrA (shown as L in Figure 2) and larger than the MsrA form that lacked the first exon (shown as S in Figure 2), suggesting that both naturally occurring mouse MsrA forms were either processed to shorter forms from the same longer protein product or were the result of internal splicing events.

Occurrence of Mitochondrial and Cytosolic Forms in Cells Transfected with MsrA-GFP Fusion Constructs. To further characterize subcellular distribution of MsrA, we generated various GFP-fusion constructs. We first tested whether MsrA was located in mitochondria and/or cytosol in transiently transfected monkey kidney CV-1 cells (Figure 3). MsrA-(1−46)-GFP (corresponded to the initial 46 amino acids of MsrA, including the mitochondrial signal, fused to GFP) co-localized with the mitochondrial marker. In contrast, MsrA-GFP (the full-length MsrA fused to GFP) was observed in cytosol and nucleus. Although this fusion form could also be seen in mitochondria, the mitochondrial location was

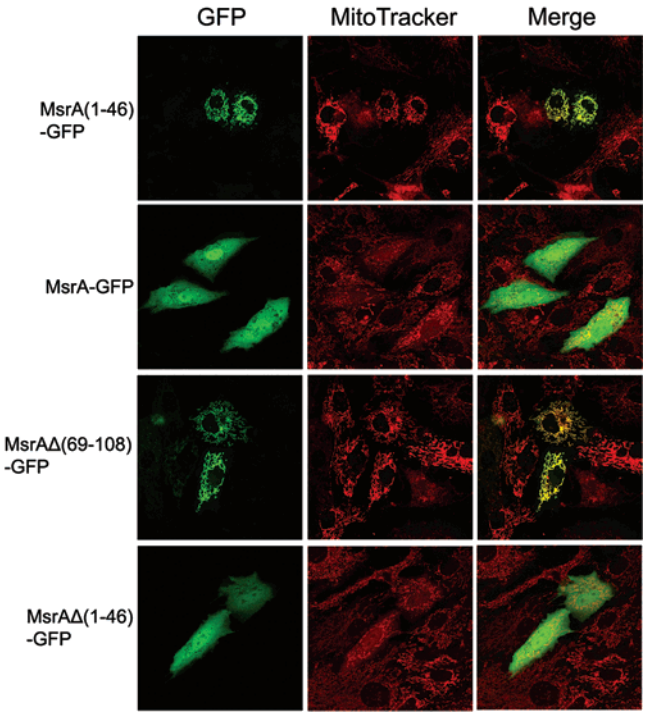

FIGURE 3: Subcellular localization of GFP-fused MsrA forms. Various GFP-fused MsrA constructs were transiently transfected into monkey kidney CV-1 cells. Fluorescence was monitored using a confocal microscope. Images at 20 h post-transfection are shown. A set of three images is shown for each construct. Left panels show green fluorescence corresponding to transiently expressed fusion proteins. Center panels show fluorescence of the mitochondrial marker (MitoTracker Red). Right panels show images obtained by merging left and center panels. The GFP fusion constructs used in each experiment are shown on the left.

largely hidden behind cytosolic and nuclear fluorescence (for example, see immunofluorescence of full-length MsrA in Figure 4). Thus, the MsrA-GFP fusion protein mimicked the occurrence and distribution of MsrA forms observed in mouse tissues. As expected, transfection of cells with mouse MsrAΔ(1−46)-GFP (amino acids 47−233 of MsrA fused to GFP), which lacked the entire first exon including the signal peptide, did not result in the mitochondrial location of the protein (Figure 3). When these data are taken together, they suggested that the N-terminal peptide was sufficient for the mitochondrial targeting (e.g., it specifically targeted GFP to mitochondria), but when present in MsrA (or in full-size MsrA fused to GFP), the localization pattern changed such that MsrA was distributed among mitochondria, cytosol, and nucleus. Thus, MsrA sequences downstream of the signal peptide were responsible for preserving a fraction of this protein for extramitochondrial compartments.

Role of Structural and Functional Elements in Subcellular Distribution. What is the determinant for such unusual distribution of MsrA in cells? To address this question, we hypothesized that there might be a sequence in MsrA, located downstream of the initial 46 amino acids, that was critical for the cytosolic location of the enzyme. We initially tested the role of the active-site region in subcellular distribution of MsrA using a deletion construct that encoded MsrAΔ-(69−108)-GFP (deletion of amino acids 69−108, which include the catalytic Gly71-Cys-Phe-Trp-Gly75 sequence of MsrA). This form corresponds to a rare EST, but we could not detect a protein product of this transcript in various mouse

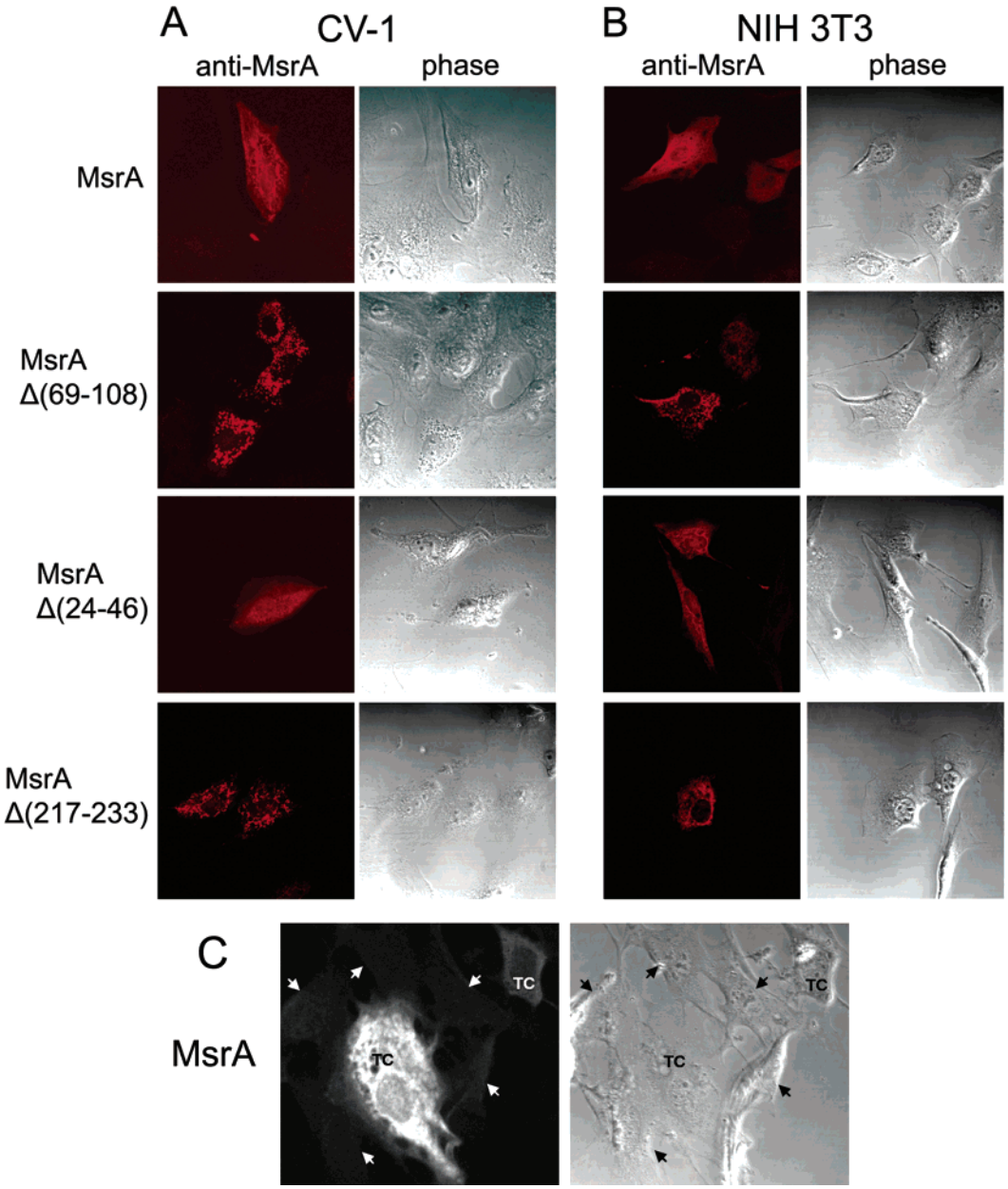

FIGURE 4: Immunofluorescence analysis of MsrA forms. Various MsrA expression constructs (without GFP fusion) were transfected into monkey kidney CV-1 cells or mouse NIH 3T3 cells. The transfected cells were stained with anti-MsrA antibodies followed by secondary anti-rabbit Cy5-conjugated antibodies. A set of two images is shown: left panel, immunofluorescence; right panel, phase contrast. (A) Images of CV-1 cells at 20 h post-transfection. (B) Images of NIH 3T3 cells at 20 h post-transfection. The constructs used in each experiment are shown on the left. (C) NIH 3T3 cells transfected with a full-length MsrA construct at 20 h post-transfection. This panel illustrates a background level and distribution of MsrA in nontransfected cells (arrows). Transfected cells are marked as TC.

tissues and cells (H.-Y. Kim and V. N. Gladyshev, unpublished data). Surprisingly, when expressed in CV-1 cells, this deletion protein was located exclusively in mitochondria (Figure 3). We could not detect this protein in cytosolic and nuclear compartments, even in cells with a very high MsrAΔ(69−108)-GFP expression.

To rule out the possibility that the mitochondrial location of MsrAΔ(69−108)-GFP was due to GFP fusion, we generated MsrA expression constructs that lacked GFP, MsrAΔGFP (full-length MsrA), and MsrAΔ(69−108)ΔGFP (deletion of amino acids 69−108 in MsrA), using the same expression vector. The constructs were transfected into CV-1 cells, and MsrA location was determined by labeling cells with polyclonal anti-MsrA antibodies followed by secondary anti-rabbit Cy5-conjugated antibodies. As shown in Figure 4A, full-length MsrA showed strong grain-like signals compatible with mitochondrial location, and the protein was also detected in cytosol and nucleus. This observation was consistent with a recent report that MsrA is localized in cytosol as well as mitochondria in human WI-38 fibroblasts (*30*). However, the deletion protein, MsrAΔ(69−108), was observed only in mitochondria. As expected, the protein that lacked the entire first exon (amino acids 1−46) was present in cytosol and nucleus (data not shown).

To further confirm this dual localization in cell culture, we generated an MsrA-His construct that encoded a protein with a C-terminal His tag. This construct was transfected into NIH 3T3 cells. Cytosolic and mitochondrial fractions were isolated from the transfected cells and subjected to Western blotting. Using anti-His antibodies, we identified

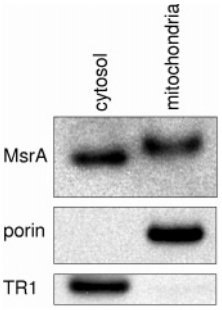

FIGURE 5: Identification of cytosolic and mitochondrial MsrA from transfected NIH 3T3 cells. Cytosolic and mitochondrial fractions were isolated from 20 h post-transfected cells with MsrA-His construct (C-terminal His-tagged), subjected to SDS−PAGE, and then transferred onto a PVDF membrane. Polyclonal anti-His antibodies were used for protein detection. Porin and thioredoxin reductase 1 (TR1) were used as mitochondrial and cytosolic markers, respectively, and were detected with the corresponding antibodies.

mitochondrial and cytosolic MsrA forms present in isolated cellular compartments (Figure 5).

Our data demonstrated that deletion of residues 69−108 prevented distribution of MsrA among cellular compartments and resulted in exclusive mitochondrial targeting of the protein. To further characterize sequences of the protein required for the cytosolic location, we generated additional deletion constructs: MsrAΔ(69−83)ΔGFP (it lacked the catalytic Gly71-Cys-Phe-Trp-Gly75 motif) and MsrAΔ(84−108)ΔGFP (the catalytic motif was included, but the residues downstream of this motif were deleted). Immunofluorescence analysis of cells expressing these constructs revealed that both protein products were targeted only to mitochondria, similarly to MsrAΔ(69−108)ΔGFP (data not shown).

Analysis of our deletion mutants against the crystal structure of bovine MsrA (*9*) showed that the segment containing amino acids 69−108 in mouse MsrA was part of the central core region, an α-β plaits motif (Figure 1). Because deletion of the core region interferes with the MsrA fold, our data were consistent with the idea that the overall structure was important for the extramitochondrial location of the protein. If this is the case, then deletions in other regions of the protein that disrupt MsrA structure could result in mitochondrial location, whereas deletions in regions that are outside of the core MsrA fold might result in the dual targeting of the protein. To test this idea, we developed the following deletion constructs: MsrAΔ(24−46)ΔGFP (deletion of residues 24−46) and MsrAΔ(217−233)ΔGFP (deletion of C-terminal residues 217−233). The former deletion protein had a mitochondrial signal, but lacked the second half of the first exon. Nevertheless, the overall MsrA fold in this protein was not expected to be disrupted (see below). The second construct lacked the C-terminal region, which was important for MsrA function because it contained catalytic residues.

As shown in Figure 4A, MsrAΔ(24−46) resided in cytosol and nucleus, and in addition, it was observed in mitochondria, similarly to the distribution of the full-length MsrA. In contrast, MsrAΔ(217−233) was observed only in mitochondria. The Cys218 residue, which was absent in the C-terminal deletion construct, is known to interact with the active-site residues and function in thiol-disulfide exchange through formation of a disulfide bond with the catalytic Cys72 (*7*, *9*). In addition, Cys227, also absent in the C-terminal deletion protein, is directly involved in the reaction mechanism by attacking the Cys72−Cys218 disulfide (*7*, *9*). Therefore, the deletion of the C-terminal residues 217−233 could be detrimental to MsrA structure and function. In contrast, residues 24−46 consisted of a loop that wrapped the central core in the bovine MsrA crystal structure. The purified MsrAΔ(1−46) protein showed significant enzyme activity (see below) (Table 1). Thus, the deletion of this N-terminal region did not appear to affect the overall MsrA structure.

Table 1: Specific Activity and Kinetic Constants of the Full-Length and the Truncated MsrA[a]

protein	specific activity [nmol min^{-1} (mg protein)$^{-1}$]	K_m (mM)	k_{cat} (s^{-1})	k_{cat}/K_m (M^{-1} s^{-1})
MsrA	238 ± 26	0.34 ± 0.04	0.28 ± 0.02	824 ± 45
MsrAΔ(1−46)	99 ± 4	4.3 ± 0.3	0.78 ± 0.03	181 ± 13

[a] Enzyme activity was determined using dabsyl-Met-*S*-SO in the presence of DTT as described in the Materials and Methods. A total of 1 μg of purified protein was used. The specific activity was determined at 200 μM dabsyl-Met-*S*-SO. For determination of K_m, the range of concentrations was from 0.05 to 0.8 mM of dabsyl-Met-*S*-SO.

We also transfected the constructs coding for various MsrA derivatives into mouse fibroblast NIH 3T3 cells (Figure 4B). The immunofluorescence analysis revealed that both full-length MsrA and MsrAΔ(24−46) localized in cytosol, nucleus, and mitochondria, whereas MsrAΔ(69−108) and MsrAΔ(217−233) were observed only in mitochondria.

Dual Targeting of a Single-Translation Product. The cytosolic form of MsrA could have resulted from alternative translation initiation at Met21, whereas the mitochondrial MsrA was synthesized from Met1 and its signal peptide was processed during translocation into mitochondria. To examine this possibility of alternative translation initiation at Met21, we mutated this residue to Ile in MsrA(1−46)-GFP, MsrA-GFP, and MsrAΔ(69−108)-GFP. The fluorescence microscopy analysis revealed that MsrA-M21I-GFP was localized in cytosol and nucleus as well as mitochondria (data not shown). However, MsrA(1−46)-M21I-GFP and MsrAΔ(69−108)-M21I-GFP were localized exclusively in mitochondria, indicating that this mutation (i) did not affect the function of the mitochondrial targeting signal and (ii) did not prevent cytosolic/nuclear location of the enzyme. Therefore, these data demonstrated that the cytosolic MsrA is not synthesized by alternative translation initiation at Met21 and that this protein form results from the processing of the full-length MsrA.

Residues 24−46 of Mouse MsrA Are Important for Substrate Binding. To investigate a possible role of residues 24−46, we expressed the C-terminal His-tagged full-length MsrA and MsrAΔ(1−46) in *E. coli* and then purified and characterized these proteins. As shown in Table 1, specific activity of full-length MsrA was 2-fold higher than that of MsrAΔ(1−46). Interestingly, the K_m value of MsrAΔ(1−46) for dabsyl-Met-*S*-SO was 12-fold higher than that of full-length MsrA, indicating that residues 24−46 are important for affinity of the enzyme for the substrate. The catalytic efficiency, k_{cat}/K_m, of MsrAΔ(1−46) was 5-fold lower than that of full-length MsrA. Our data were consistent with the observation that the N-terminal truncated (residues 1−41)

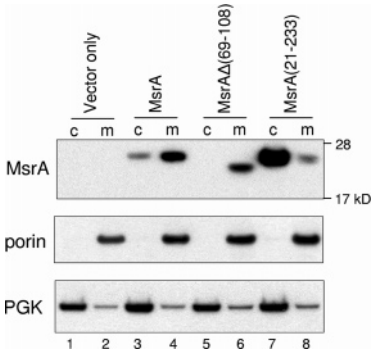

FIGURE 6: Dual targeting of mouse MsrA in *S. cerevisiae*. Mitochondrial and cytosolic fractions were isolated from yeast GY4 cells expressing mouse MsrA genes as described in the Materials and Methods. A total of 10 μg of cytosolic and 2.5 μg of mitochondrial proteins were subjected to SDS−PAGE and Western blotting for MsrA detection with anti-MsrA antibodies. Porin and 3-phosphoglycerate kinase (PGK) were used as mitochondrial and cytosolic markers, respectively, and detected with corresponding antibodies. Lanes 1 and 2, cytosolic (c) and mitochondrial (m) fractions isolated from cells expressing an empty p423 vector, respectively; lanes 3 and 4, cytosolic (c) and mitochondrial (m) fractions from cells expressing full-length MsrA; lanes 5 and 6, cytosolic (c) and mitochondrial (m) fractions from cells expressing MsrAΔ(69−108); and lanes 7 and 8, cytosolic (c) and mitochondrial (m) fractions from cells expressing MsrA(21−233).

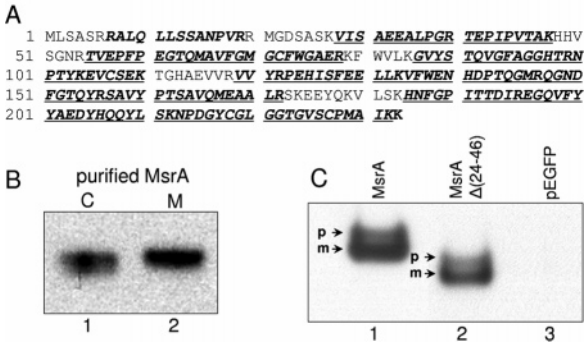

FIGURE 7: Post-translational translocation of MsrA into mitochondria. (A) Identification of MsrA peptides purified from yeast cells by MS/MS analysis. Peptides, whose sequences were determined by MS/MS are shown in bold. Peptides identified in the cytosolic fraction are shown in italics. Peptides identified in both cytosolic and mitochondrial fractions are underlined. (B) Western blot analysis of mouse MsrA-His purified from yeast subcellular fractions. Polyclonal anti-MsrA antibodies were used for protein detection. Lane 1, cytosolic fraction; and lane 2, mitochondrial fraction. (C) Western blot analysis of MsrA products in transfected NIH 3T3 cells. Whole-cell extracts at 20 h post-transfection were subjected to SDS−PAGE and Western blotting with polyclonal anti-MsrA antibodies. Precursor (upper band) and mature (lower band) forms from full-length MsrAΔGFP (lane 1) and MsrAΔ(24−46)ΔGFP (lane 2) constructs are indicated by arrows. Endogenous MsrA proteins were not detectable under these experimental conditions (lane 3).

E. coli MsrA exhibited 4-fold higher K_m and 6-fold lower k_{cat}/K_m values than the full-length enzyme (*31*).

Dual Targeting of Mouse MsrA in S. cerevisiae. Is the mechanism responsible for distribution of MsrA among different cellular compartments specific for mammalian cells or conserved in other species? To test if the dual targeting may occur in yeast cells, we expressed full-length mouse MsrA, MsrAΔ(69−108), and MsrA(21−233) forms in *S. cerevisiae* cells lacking the endogenous MsrA. The cytosolic and mitochondrial fractions were isolated from the cells expressing these MsrA forms grown in synthetic medium supplemented with D,L-lactate as a carbon source. As shown in Figure 6, full-length mouse MsrA was localized in both cytosol and mitochondria (lanes 3 and 4). However, the deletion mutant, MsrAΔ(69−108), was located exclusively in mitochondria (lane 6). The MsrA band was not detected in the cytosolic fraction (lane 5) even after a long exposure time (data not shown). As expected, MsrA(21−233) that lacked the mitochondrial target signal was localized in the cytosol (lane 7). A weak band of MsrA(21−233) was detected in the mitochondrial fraction, but this was due to minor cytosolic contamination (lane 8). Our data suggested that mammalian and yeast cells share a common mechanism for dual targeting of MsrA and that, in each case, proper structure−function organization of MsrA played an important role in its subcellular localization.

Subcellular Distribution of MsrA Occurs Post-translationally. We attempted purification of cytosolic and mitochondrial MsrAs containing C-terminal His tag after large-scale transfection of NIH 3T3 cells but could not obtain sufficient amounts for comparative analyses of the two forms. Instead, purification of each form was achieved from yeast cells overexpressing His-tagged MsrA (Figure 7B). The purified forms were subjected to SDS−PAGE and in-gel digestion with trypsin, and the resulting peptides were sequenced by LC−MS/MS. The sequenced tryptic peptides covered 79% (cytosolic protein) and 74% (mitochondrial protein) of the theoretical MsrA sequence (Figure 7A). Same sequences were detected for cytosolic and mitochondrial forms downstream of Val28. Interestingly, a tryptic peptide corresponding to residues 7−19 was detected in the cytosolic MsrA. Its occurrence suggested that a precursor containing a signal peptide was present in the purified cytosolic MsrA fraction. These data were consistent with the idea that the full-size form of MsrA was initially synthesized in the yeast cytosol following translocation of the protein in mitochondria. The precursor form was also observed in the whole-cell extracts of NIH 3T3 cells transfected with full-length MsrA and MsrAΔ(24−46) constructs (Figure 7C, upper bands). Overall, these data suggested that distribution of MsrA among cellular compartments was a post-translational event, as opposed to the co-translational synthesis of MsrA targeted to mitochondria.

DISCUSSION

In the present study, we localized MsrA in mouse cells and tissues and identified elements important for MsrA structure and function as key factors that determine subcellular distribution of MsrA forms. The mouse protein was found to reside in cytosol, nucleus, and mitochondria. The N-terminal signal peptide of MsrA was responsible for the mitochondrial location of the enzyme and could also target GFP to this cellular compartment. In addition, removal of residues 69−108, 69−83, 84−108, or 217−233, which contained critical structural elements of MsrA, led to the exclusive mitochondrial location of MsrA. However, deletion of residues 24−46, which influenced catalytic efficiency of the enzyme but did not affect the overall structure, resulted in cytosolic and nuclear forms as well as in the mitochondrial protein. We also excluded the possibility that alternative translation initiation produces MsrA forms destined for different compartments. We concluded that the default

function of the N-terminal signal peptide of MsrA was mitochondrial targeting, but proper structural organization of MsrA was required for its cytosolic and nuclear location.

On the basis of our study and an earlier report (*25*), we propose that the major naturally occurring MsrA forms result from subcellular distribution of a protein containing a mitochondrial signal peptide rather than products of alternative splicing. However, we also detected an alternative splicing form of this protein that lacks the mitochondrial signal peptide (H.-Y. Kim and V. N. Gladyshev, unpublished data). This form is generated from an alternative first exon; however, it is not abundant, and its transcript appears to be present in detectable levels only in some tissues. Moreover, alternative splicing of MsrA genes can be seen in other animals, including insects (H.-Y. Kim and V. N. Gladyshev, unpublished data).

The details of the molecular mechanism, which allows MsrA containing the N-terminal signal peptide to be targeted to cytosol and nucleus, in addition to mitochondria, are unclear. However, our data revealed that there is a common mechanism for the dual targeting of MsrA in mammals and yeast. Our study also suggested that the translocation of MsrA into mitochondria is a post-translational event. It is possible that there might be a regulatory signal(s) for MsrA subcellular distribution, such as an increase in the levels of mitochondrial MsrA over a certain limit or an overall redox status of mitochondria or other compartments.

The mature form of cytosolic MsrA, like that in mitochondria, lacked the N-terminal signal sequence. Interestingly, this form often migrated faster than the mitochondrial form on SDS−PAGE gels, suggesting either further processing of the cytosolic protein or a post-translational modification of the mitochondrial form. We were not able to identify differences between the two forms by MS/MS analyses.

MsrAΔ(69−108) localized exclusively in mitochondria in transfected mammalian cells and was also detected exclusively in the mitochondrial fraction in *S. cerevisiae* cells expressing this protein form. It could not be excluded that the mitochondrial form of MsrAΔ(69−108) was highly stable, whereas the cytosolic form was rapidly degraded; however, because this distribution of MsrA forms between different compartments was reproduced with various deletion constructs and in two different model organisms, this possibility is viewed as unlikely.

There are two possible models to explain the unusual cellular distribution pattern of MsrA. One model would invoke a retrograde transport of the protein from mitochondria. In this model, MsrA would be synthesized in the cytosol and the precursor protein would be maintained in a partially unfolded state by chaperones. This form of the MsrA preprotein would be imported into mitochondria post-translationally, concurrent with the cleavage of the N-terminal signal peptide. However, depending on a folding state of the protein or folding-dependent regulatory events, a fraction of the mature protein would be transported back to the cytosol. The MsrA exported to cytosol would not be able to re-enter mitochondria because of the lack of the targeting signal. The cytosolic form could then be translocated into the nucleus.

The second model would be consistent with the competitive folding of the precursor protein in the cytosol. After the synthesis of MsrA in the cytosol, a fraction of the precursor protein would undergo folding to become unable to translocate into mitochondria. The folded cytosolic protein would then be processed into a mature form, in which the N-terminal region is removed by unknown proteases. The remaining partially unfolded precursors should be imported into mitochondria by the mitochondrial signal peptide. Mass spectrometry analyses of rat (*25*) and mouse (our study) MsrA revealed sequences from Val28 to the C terminus in both cytosolic and mitochondrial forms. However, we found that MsrAΔ(24−46) could result in the cytosolic form. Therefore, if the precursor is truncated in the cytosol, the site would be between the signal peptide cleavage site (Met21 as predicted by MitoProt) and Asp23.

It has been reported that a limited number of proteins synthesized as single-translation products could be distributed between mitochondria and extramitochondrial fractions (*32*−*34*), but mammalian proteins that are targeted to mitochondria and cytosol by processing of common N-terminal sequences are not known. In addition, molecular details of the dual targeting of proteins in cytosol and mitochondria have not been clearly established. Strobel et al. (*35*) reported that competition between spontaneous protein folding and mitochondrial import of yeast adenylate kinase (Aky2) determines its location in cytosol and mitochondria. Yeast fumarase is also distributed between mitochondria and cytosol, but the mechanism is different because the protein shows retrograde transport back to the cytosol (*33*, *36*). Fumarase is synthesized as a single-translation product, co-translationally targeted to mitochondria by a typical amphipathic presequence at the N terminus, and subsequently, a fraction of the processed protein is transported back to the cytosol. More recently, Sass et al. (*37*) reported that folding of fumarase is involved in its cytosolic and mitochondrial location in yeast. Our finding that proper structural organization of mouse MsrA regulates its subcellular distribution is consistent with the previous data on fumarase and Aky2 and suggests that these mechanisms may also operate in mammals.

Only a single mammalian MsrA gene is known, whereas human and mouse genomes possess three MsrB genes, whose products reside in different cellular compartments (cytosolic and nuclear MsrB1, mitochondrial MsrB2, and ER-resident MsrB3). The structure- or folding-dependent distribution of MsrA provides a mechanism to target MsrA to various cellular compartments. The presence of MsrA in mitochondria, cytosol, and nucleus may complement the occurrence of MsrB proteins in these compartments. An exception would be the ER. MsrA has neither an ER signal peptide nor a C-terminal ER retention signal. It is not clear whether MsrA is targeted to the ER via an unknown mechanism or if there is a replacement for the MsrA function in the ER (e.g., an enzyme with either MsrA or methionine sulfoxide epimerase activity; the latter could convert Met-*S*-SO to Met-*R*-SO to be accessible for MsrB3). It is also possible that the ER lacks the MsrA function altogether.

ACKNOWLEDGMENT

We thank Bertrand Friguet for providing anti-MsrA antibodies.

REFERENCES

1. Weissbach, H., Etienne, F., Hoshi, T., Heinemann, S. H., Lowther, W. T., Matthews, B., St. John, G., Nathan, C., and Brot, N. (2002)

Peptide methionine sulfoxide reductase: Structure, mechanism of action, and biological function, *Arch. Biochem. Biophys. 397*, 172−178.
2. Levine, R. L., Moskovitz, J., and Stadtman, E. R. (2000) Oxidation of methionine in proteins: Roles in antioxidant defense and cellular regulation, *IUBMB Life 50*, 301−307.
3. Stadtman, E. R., Moskovitz, J., and Levine, R. L. (2003) Oxidation of methionine residues of proteins: Biological consequences, *Antioxid. Redox Signaling 5*, 577−582.
4. Hoshi, T., and Heinemann, S. H. (2001) Regulation of cell function by methionine oxidation and reduction, *J. Physiol. 531.1*, 1−11.
5. Brot, N., Weissbach, L., Werth, J., and Weissbach, H. (1981) Enzymatic reduction of protein-bound methionine sulfoxide, *Proc. Natl. Acad. Sci. U.S.A. 78*, 2155−2158.
6. Brot, N., and Weissbach, H. (1983) Biochemistry and physiological role of methionine sulfoxide residues in proteins, *Arch. Biochem. Biophys. 223*, 271−281.
7. Lowther, W. T., Brot, N., Weissbach, H., Honek, J. F., and Matthews, B. W. (2000) Thiol-disulfide exchange is involved in the catalytic mechanism of peptide methionine sulfoxide reductase, *Proc. Natl. Acad. Sci. U.S.A. 97*, 6463−6468.
8. Moskovitz, J., Poston, J. M., Berlett, B. S., Nosworthy, N. J., Szczepanowski, R., and Stadtman, E. R. (2000) Identification and characterization of a putative active site for peptide methionine sulfoxide reductase (MsrA) and its substrate stereospecificity, *J. Biol. Chem. 275*, 14167−14172.
9. Lowther, W. T., Brot, N., Weissbach, H., and Matthews, B. W. (2000) Structure and mechanism of peptide methionine sulfoxide reductase, an "anti-oxidation" enzyme, *Biochemistry 39*, 13307−13312.
10. Moskovitz, J., Weissbach, H., and Brot, N. (1996) Cloning the expression of a mammalian gene involved in the reduction of methionine sulfoxide residues in proteins, *Proc. Natl. Acad. Sci. U.S.A. 93*, 2095−2099.
11. Kuschel, L., Hansel, A., Schonherr, R., Weissbach, H., Brot, N., Hoshi, T., and Heinemann, S. H. (1999) Molecular cloning and functional expression of a human peptide methionine sulfoxide reductase (hMsrA), *FEBS Lett. 456*, 17−21.
12. Antoine, M., Boschi-Muller, S., and Branlant, G. (2003) Kinetic characterization of the chemical steps involved in the catalytic mechanism of methionine sulfoxide reductase A from *Neisseria meningitides*, *J. Biol. Chem. 278*, 45352−45357.
13. Grimaud, R., Ezraty, B., Mitchell, J. K., Lafitte, D., Briand, C., Derrick, P. J., and Barras, F. (2001) Repair of oxidized proteins. Identification of a new methionine sulfoxide reductase, *J. Biol. Chem. 276*, 48915−48920.
14. Jung, S., Hansel, A., Kasperczyk, H., Hoshi, T., and Heinemann, S. H. (2002) Activity, tissue distribution, and site-directed mutagenesis of a human peptide methionine sulfoxide reductase of type B: hCBS1, *FEBS Lett. 527*, 91−94.
15. Kryukov, G. V., Kumar, R. A., Koc, A., Sun, Z., and Gladyshev, V. N. (2002) Selenoprotein R is a zinc-containing stereo-specific methionine sulfoxide reductase, *Proc. Natl. Acad. Sci. U.S.A.* 99, 4245−4250.
16. Kumar, R. A., Koc, A., Cerny, R. L., and Gladyshev, V. N. (2002) Reaction mechanism, evolutionary analysis, and role of zinc in *Drosophila* methionine-*R*-sulfoxide reductase, *J. Biol. Chem. 277*, 37527−37535.
17. Olry, A., Boschi-Muller, S., Marraud, M., Sanglier-Cianferani, S., van Dorsselear, A., and Branlant, G. (2002) Characterization of the methionine sulfoxide reductase activities of PILB, a probable virulence factor from *Neisseria meningitides*, *J. Biol. Chem. 277*, 12016−12022.
18. Lowther, W. T., Weissbach, H., Etienne, F., Brot, N., and Matthews, B. W. (2002) The mirrored methionine sulfoxide reductases of *Neisseria gonorrhoeae* pilB, *Nat. Struct. Biol. 9*, 348−352.
19. Spector, D., Etienne, F., Brot, N., and Weissbach, H. (2003) New membrane-associated and soluble peptide methionine sulfoxide reductases in *Escherichia coli*, *Biochem. Biophys. Res. Commun. 302*, 284−289.
20. Kim, H. Y., and Gladyshev, V. N. (2004) Methionine sulfoxide reduction in mammals: Characterization of methionine-*R*-sulfoxide reductases, *Mol. Biol. Cell 15*, 1055−1064.
21. Lescure, A., Gautheret, D., Carbon, P., and Krol, A. (1999) Novel selenoproteins identified *in silico* and *in vivo* by using a conserved RNA structural motif, *J. Biol. Chem. 274*, 38147−38154.
22. Huang, W., Escribano, J., Sarfarazi, M., and Coca-Prados, M. (1999) Identification, expression, and chromosome localization of a human gene encoding a novel protein with similarity to the pilB family of transcriptional factors (pilin) and to bacterial peptide methionine sulfoxide reductases, *Gene 233*, 233−240.
23. Kim, H. Y., and Gladyshev, V. N. (2004) Characterization of mouse endoplasmic reticulum methionine-*R*-sulfoxide reductase, *Biochem. Biophys. Res. Commun. 320*, 1277−1283.
24. Hansel, A., Kuschel, L., Hehl, S., Lemke, C., Agricola, H. J., Hoshi, T., and Heinemann, S. H. (2002) Mitochondrial targeting of the human peptide methionine sulfoxide reductase (MSRA), an enzyme involved in the repair of oxidized proteins, *FASEB J. 16*, 911−913.
25. Vougier, S., Mary, J., and Friguet, B. (2003) Subcellular localization of methionine sulphoxide reductase A (MsrA): Evidence for mitochondrial and cytosolic isoforms in rat liver cells, *Biochem. J. 373*, 531−537.
26. Makarova, O., Kamberov, E., and Margolis, B. (2000) Generation of deletion and point mutations with one primer in a single cloning step, *BioTechniques 29*, 970−972.
27. Mumberg, D., Muller, R., and Funk, M. (1995) Yeast vectors for the controlled expression of heterologous proteins in different genetic backgrounds, *Gene 156*, 119−122.
28. Daum, G., Bohni, P. C., and Schatz, G. (1982) Import of proteins into mitochondria. Cytochrome *b*2 and cytochrome *c* peroxidase are located in the intermembrane space of yeast mitochondria, *J. Biol. Chem. 257*, 13028−13033.
29. Hansel, A., Jung, S., Hoshi, T., and Heinemann, S. H. (2003) A second human methionine sulfoxide reductase (hMSRB2) reducing methionine-*R*-sulfoxide displays a tissue expression pattern distinct from hMSRB1, *Redox Rep. 8*, 384−388.
30. Picot, C. R., Perichon, M., Cintrat, J. C., Friguet, B., and Petropoulos, I. (2004) The peptide methionine sulfoxide reductases, MsrA and MsrB (hCBS-1), are downregulated during replicative senescence of human WI-38 fibroblasts, *FEBS Lett. 558*, 74−78.
31. Boschi-Muller, S., Azza, S., and Branlant, G. (2001) *E. coli* methionine sulfoxide reductase with a truncated N terminus or C terminus, or both, retains the ability to reduce methionine sulfoxide, *Protein Sci. 10*, 2272−2279.
32. Soltys, B. J., and Gupta, R. S. (1999) Mitochondrial-matrix proteins at unexpected locations: Are they exported? *Trends Biochem. Sci. 24*, 174−177.
33. Stein, I., Peleg, Y., Even-Ram, S., and Pines, O. (1994) The single translation product of the FUM1 gene (fumarase) is processed in mitochondria before being distributed between the cytosol and mitochondria in *Saccharomyces cerevisiae*, *Mol. Cell. Biol. 14*, 4770−4778.
34. Anandatheerthavarada, H. K., Biswas, G., Mullick, J., Sepuri, N. B., Otvos, L., Pain, D., and Avadhani, N. G. (1999) Dual targeting of cytochrome P4502B1 to endoplasmic reticulum and mitochondria involves a novel signal activation by cyclic AMP-dependent phosphorylation at Ser128, *EMBO J. 18*, 5494−5504.
35. Strobel, G., Zollner, A., Angermayr, M., and Bandlow, W. (2002) Competition of spontaneous protein folding and mitochondrial import causes dual subcellular location of major adenylate kinase, *Mol. Biol. Cell 13*, 1439−1448.
36. Sass, E., Blachinsky, E., Karniely, S., and Pines, O. (2001) Mitochondrial and cytosolic isoforms of yeast fumarase are derivatives of a single translation product and have identical amino termini, *J. Biol. Chem. 276*, 46111−46117.
37. Sass, E., Karniely, S., and Pines, O. (2003) Folding of fumarase during mitochondrial import determines its dual targeting in yeast, *J. Biol. Chem. 278*, 45109−45116.

BI0501131